

Two-Dimensional Planing in Water of Finite Depth

Zhihang Zhang

Department of Naval Architecture and Marine Engineering
University of Michigan, Ann Arbor, USA
ZhihangZ@Umich.edu

Kevin J. Maki

Department of Naval Architecture and Marine Engineering
University of Michigan, Ann Arbor, USA
KJMaki@UMich.edu

Lawrence J. Doctors

School of Mechanical and Manufacturing Engineering
The University of New South Wales, Sydney, Australia
L.Doctors@UNSW.edu.au

Highlights

The traditional deep-water analysis of planing is extended to the case where the water has a finite depth. There are remarkable and strong depth phenomena, which are predicted by the potential-flow and the computational fluid dynamics analyses. Furthermore, the formulation of Newman and Poole (1962, Equation 10) is shown to apply to the sudden drop in the wave-resistance component of the total inviscid drag at the critical speed.

1 Introduction

A detailed summary of the early work by Sedov (1936), Maruo (1951), Maruo (1956), Maruo (1957), Maruo (1959), Squire (1957) and Sedov (1965, Chapter VII), can be found in the work of Doctors (1974).

In all cases, the planing surface is represented by an unknown pressure distribution, which is to be found. Doctors (1974) developed a simple approach in which the pressure is composed of overlapping triangular elements, as depicted in Figure 1(a).

Here we extend the work to include the effects of finite depth and we complement the results with computational fluid dynamics (CFD).

2 Potential-Flow Theory

We follow the classic inviscid-flow approach and assume linearized kinematic and dynamic conditions at the free surface, as well as the kinematic condition on the bottom. The wave elevation for a pressure patch was given by Doctors (2018a, Equation 12.12). For the current application, we only require the zeroth (transverse or two-dimensional) term in the summation of the wave components:

$$\zeta(x) = \frac{1}{\pi} \int_0^{\infty} dk k^2 \exp(ikx) \mathcal{U}/f - \left\langle ik^2 \exp(ikx) \mathcal{U} / \frac{df}{dk} \right\rangle - \delta(x), \quad (1)$$

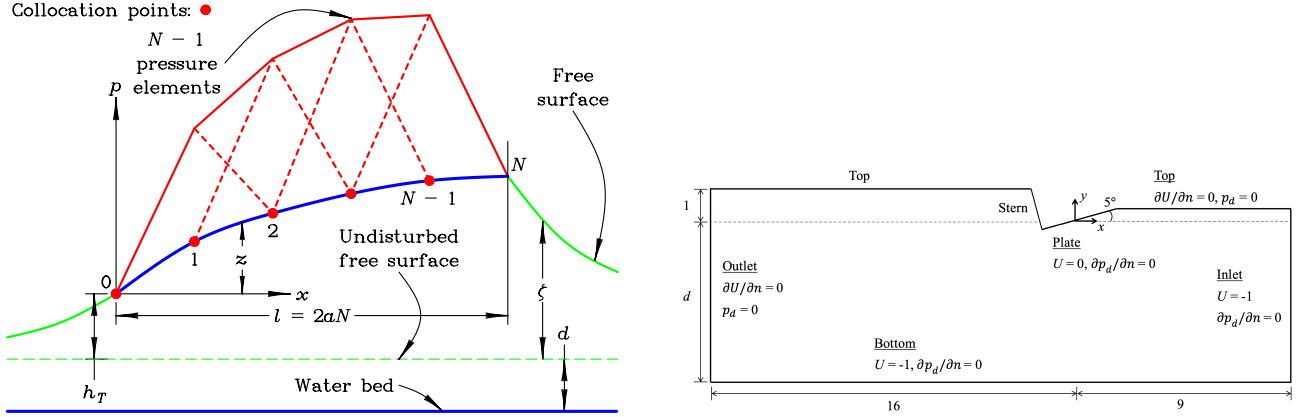
$$f = k^2 - k_0 k \tanh(kd), \quad (2)$$

$$df/dk = 2k - k_0 \tanh(kd) - k_0 kd \operatorname{sech}^2(kd), \quad (3)$$

$$k_0 = g/U^2, \quad (4)$$

where k is the wave number, f is the dispersion relationship and k_0 is the fundamental circular wave number. Equation 1 applies only to a pressure element which is symmetric fore-and-aft – as in the present case. The static depression in Equation 1 is $\delta(x)$.

The solution for k in the implicit equation for $f = 0$ in Equation 2 can be found in the usual way by using the Newton-Raphson iteration with the assistance of its derivative in Equation 3. For



(a) Triangular Pressure Elements

(b) Computational Domain

Figure 1: Definition of the Problem

subcritical speeds, $F_d = U/\sqrt{gd} < 1$, the second term in Equation 1 is evaluated for this solution. For supercritical speeds there is no solution and this term is to be ignored; this is indicated by the $\langle \rangle$ notation.

The Kochin function \mathcal{U} for a triangular element was given by Doctors (2018b, Section 8.3) as

$$\mathcal{U} = \delta_0 \cdot 2a \cdot [\sin(ka)/ka]^2, \quad (5)$$

in which δ_0 is the nominal (peak) static depression for the pressure element.

3 Results for Influence Function

The influence function in Equation 1 for various test cases has been checked with the deep-water analytic formula developed by Doctors (1974). It has also been verified for the case of finite water depth with the work of Maki, Broglia, Doctors and Di Mascio (2012).

4 Computational Fluid Dynamics

A two-phase flow solver, which is based on the open-source CFD library OpenFOAM, is used to model the nonlinear viscous-fluid flow around the planing plate. The Reynolds-averaged Navier-Stokes (RANS) equations are used to govern both the water and air.

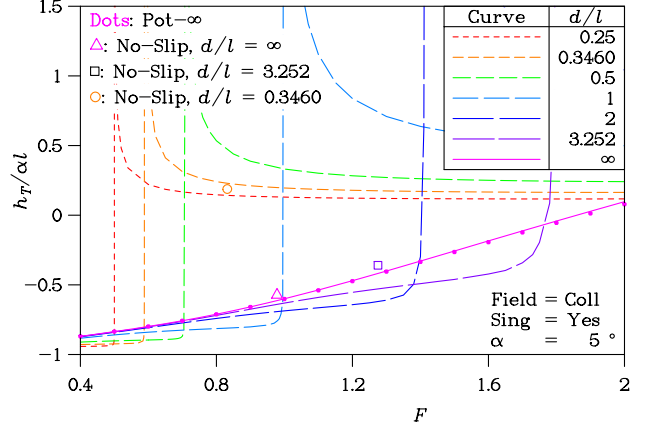
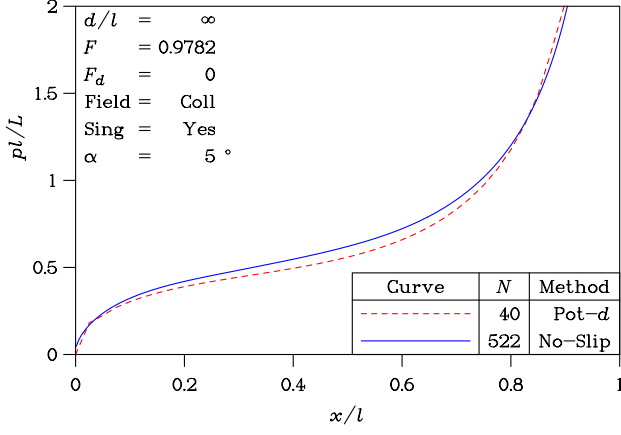
Figure 1(b) shows the computational domain with boundary conditions and dimensions. For the present simulations, the flow speed $U = 1$, gravity $g = 1$, and trim angle $\alpha = 5^\circ$ are fixed. Three different water depths are studied; $d = 16, 2$, and 0.5 . Other fluid parameters include the water density $\rho = 998.8$, air density $\rho_a = 1$, water kinematic viscosity $\nu = 1.09 \times 10^{-6}$ and air kinematic viscosity $\nu_a = 1.48 \times 10^{-5}$.

Other details of the solver and numerical setup can be found in Garland and Maki (2012) and Kramer, Maki and Young (2013).

5 Results for Planing

The pressure distribution p in Figure 2(a) has been nondimensionalized using the wetted length l and the lift L . The finite-depth potential-flow method is compared with the CFD data using the no-slip boundary condition. The Froude number F based on the wetted length is not a selected round number, because this length is not prescribed in the CFD method.

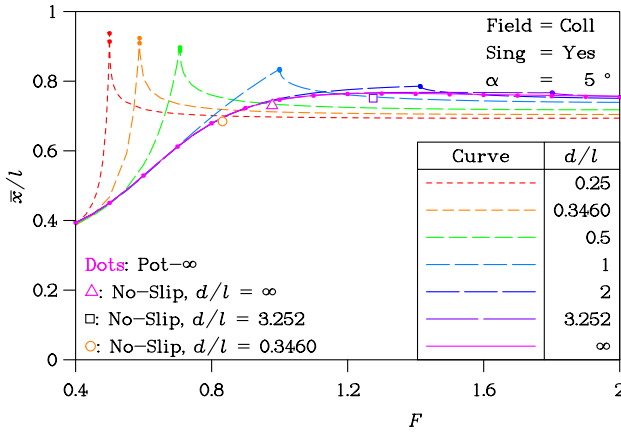
The dimensionless trailing-edge elevation is plotted against the Froude number for a selection of dimensionless depths d/l in Figure 2(b). The singular behavior of the elevation in the region near the critical speed is evident. It is pleasing to see the close agreement between the potential-flow predictions and the three CFD-computed points. In particular, the bizarre result of a positive trailing-edge elevation for the relatively-shallow-water case of $d/l = 0.3460$ is confirmed.



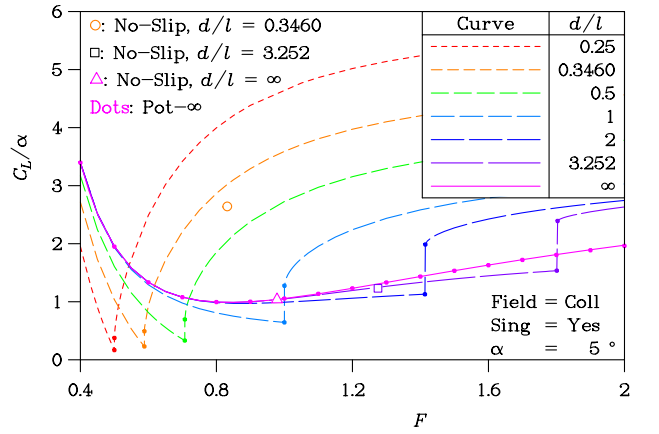
(a) Pressure

(b) Trailing-Edge Elevation

Figure 2: Pressure Distribution and Trailing-Edge Elevation



(a) Center of Pressure



(b) Lift

Figure 3: Center of Pressure and Lift

The dots represent data from the deep-water-only method described by Doctors (1974). They provide confirmation of the coding in the new finite-depth software.

The dimensionless center of pressure \bar{x}/l is plotted in Figure 3(a). The potential-flow predictions indicate that there is extreme, but not singular, behavior near the critical speed. Once again, the CFD deep-water and finite-depth points lie extremely close to the potential-flow curves.

The lift coefficient per unit trim angle C_L/α is shown in Figure 3(b). There is a sudden rise in the lift at the critical speed. The CFD deep-water point falls slightly below the potential-flow curve. The two finite-depth CFD data points are in very close agreement with the potential-flow predictions.

The potential-flow wave-resistance coefficient is plotted in Figure 4(a). The wave resistance drops to zero at the critical speed because this is a two-dimensional problem.

This sudden drop is related to the loss of the second term in Equation 1. It was first discovered by Newman and Poole (1962, Equation 10) for a pressure distribution. The same result was derived by Doctors (2018b, Section 5.5) for a displacement vessel with weight W in a channel of width w :

$$\Delta R_W = \frac{3W^2}{2\rho g w d^2} \text{ with } w \equiv 1. \quad (6)$$

Here we can substitute $W = L = \frac{1}{2}\rho U^2 l \cdot C_L$ and $R_W = \frac{1}{2}\rho U^2 l \cdot C_W$ into Equation 6. We also note that $F_d = 1$ and $w \equiv 1$. After some algebra it can be show that

$$\Delta C_W/C_L^2 = (3/4) \cdot (l/d). \quad (7)$$

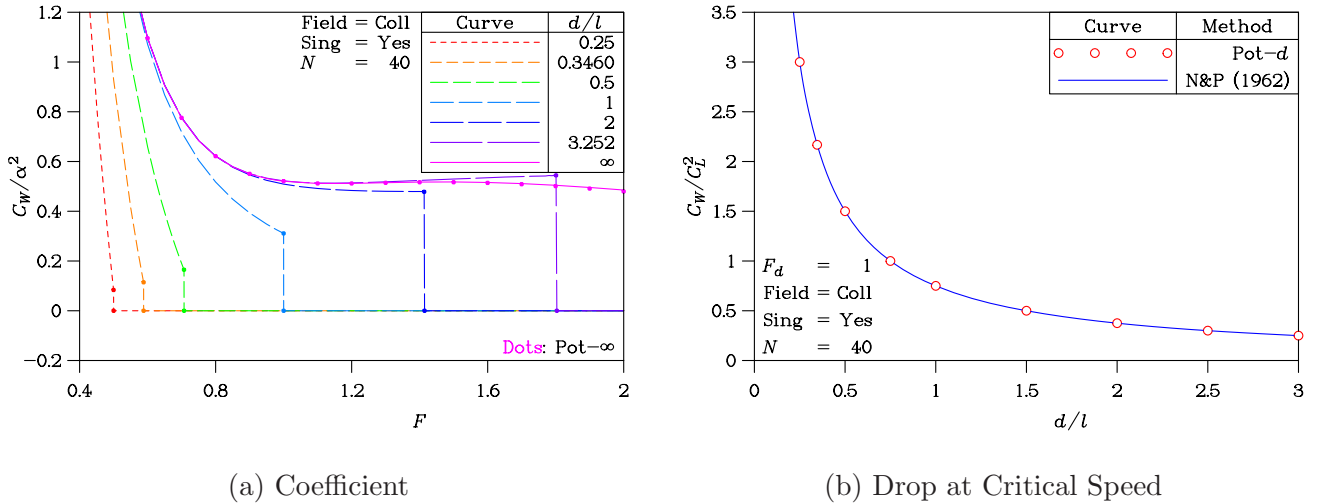


Figure 4: Wave Resistance

The two sides of Equation 7 are plotted in Figure 4(b) and this remarkable phenomenon is verified for the planing case. However, we note that the planing surface also generally suffers spray resistance, which is to be considered separately.

6 Concluding Comments

Further work is required to resolve the minor discrepancies between the predictions of the lift between the potential-flow and the CFD calculations. The differences might be attributed to nonlinear effects and the presence of viscosity in the CFD analysis.

Long-term plans include extension of this work to the three-dimensional case.

7 References

- Doctors, L. J. (1974): “Representation of Planing Surfaces by Finite Pressure Elements”, *Proc. Fifth Australasian Conference on Hydraulics and Fluid Mechanics*, Christchurch, New Zealand, Vol. 2, pp 480–488, December.
- Doctors, L. J. (2018a): *Hydrodynamics of High-Performance Marine Vessels*, Printed by CreateSpace, an Amazon.com Company, Charleston, South Carolina, Second Edition, Vol. 2, pp 423–885+ii, January.
- Doctors, L. J. (2018b): *Hydrodynamics of High-Performance Marine Vessels*, Printed by CreateSpace, an Amazon.com Company, Charleston, South Carolina, Second Edition, Vol. 1, pp 1–421+li, January.
- Garland, W. R. and Maki, K. J. (2012): “A Numerical Study of a Two-Dimensional Stepped Planing Surface”, *J. Ship Production and Design*, Vol. 28, No. 2, pp 60–72, May.
- Kramer, M. R., Maki, K. J., and Young, Y. L. (2013): “Numerical Prediction of the Flow Past a 2-D Planing Plate at Low Froude Number”, *Ocean Engineering*, Vol. 70, pp 110–117, September.
- Maki, K. J., Broglia, R., Doctors, L. J., and Di Mascio, A. (2012): “Nonlinear Wave Resistance of a two-Dimensional Pressure Patch Moving on a Free Surface”, *Ocean Engineering*, Vol. 39, pp 62–71, January.
- Maruo, H. (1951): “Two Dimensional Theory of the Hydroplane”, *Proc. First Japan National Congress for Applied Mechanics*, pp 409–415.
- Maruo, H. (1956): “Hydrodynamic Researches of the Hydroplane (Part 1)”, *J. Zosen Kiokai*, Vol. 91, pp 9–16, September.
- Maruo, H. (1957): “Hydrodynamic Researches of the Hydroplane (Part 2)”, *J. Zosen Kiokai*, Vol. 92, pp 57–63, April.
- Maruo, H. (1959): “Hydrodynamic Researches of the Hydroplane (Part 3)”, *J. Zosen Kiokai*, Vol. 105, pp 23–26, July.
- Newman, J. N. and Poole, F. A. P. (1962): “The Wave Resistance of a Moving Pressure Distribution in a Canal”, *Schiffstechnik*, Vol. 9, No. 45, pp 21–26, January.
- Sedov, L. I. (1936): “Two Dimensional Problem of Planing on the Surface of a Heavy Fluid”, *Trudy Konferentsii po Teorii Volnovogo Sprotivleniya*, Moscow, pp 7–30.
- Sedov, L. I. (1965): *Two-Dimensional Problems in Hydrodynamics and Aerodynamics*, Interscience Publishers, New York, NY, Translated from the Russian and edited by Chu, C.K., Cohen, H., and Seckler, B., 427+xv pp.
- Squire, H. B. (1957): “The Motion of a Simple Wedge along the Water Surface”, *Proc. Royal Society of London, Series A*, Vol. 243, No. 1232, pp 48–64, December.